Proceedings of the 5th International Conference on Nanotechnology: Fundamentals and Applications
Prague, Czech Republic, August 11-13, 2014
Paper No. 95

Charge Transfer Effects on Ferromagnetism of Vacancy-defect Bi-layer Graphenes

Shih-Jye Sun
Department of Applied Physics, National University of Kaohsiung
No.700, Kaohsiung University Road. Nan-Tzu District, Kaohsiung 81148, Taiwan
sjs@nuk.edu.tw

Son-Hsien Chen
University of Taipei, Department of Applied Physics and Chemistry
No.1, Aiguo W. Road, Zhongzheng District, Taipei 10048, Taiwan
sonhisen@gmail.com

Abstract - The vacancy-defect bi-layer graphene has been theoretically confirmed to have the ferromagnetism which would exhibit from the atomic sites around the vacancy defects. The purpose of the research is to investigate external and internal charge transfer effects on the ferromagnetism induced from the vacancy-defects, respectively. The calculations in the study show that the external charge transfer, in either positive or negative doping, will sensitively suppress the ferromagnetism. On the contrary, the internal charge transfer hardly makes any change to the ferromagnetism.

1. Introduction

Carbon based materials are anticipated as the candidate of the next generation of electronic (Avouris et al., 2007). Graphene reveals both excellent properties in extremely high conductivity and long spin coherent length, because of the massless conduction carriers in the Dirac linear bands and the relatively small spin-orbit coupling from its light molecular weight, respectively (Castro et al., 2009; Novoselov et al., 2005). If the graphene can exhibit the ferromagnetism, it will become a good candidate material for the carbon based spintronics (Tombros et al., 2007; Haugen et al., 2008; Yazyev, et al., 2008). Up to now, scientists propose diverse methods to induce the ferromagnetism in graphene (Kan et al., 2008), e.g., doping magnetic ions (Dugaev et al., 2006; Santos et al., 2010) or non-magnetic ions (Wu et al., 2008), creating structure defects (Palacios et al., 2008; Esquinazi et al., 2003; Nair et al., 2012), etc. The ferromagnetism appearing on the zigzag edges of ribbon is one inspiration of the magnetism induction in graphene. Eventually, the magnetism was confirmed from the ”localized” edge states (Joley et al., 2010; Uchoa et al., 2008; Fujita et al., 1996; Kumazaki, Hirashima, 2008; Soon et al., 2006). Similarly, a single layer graphene with point defects will also be predicted to exhibit the ferromagnetism in case of similar edges around the point defects. These approaches have been theoretically employed to investigate the appearance of ferromagnetism around the point defects (Sun, Magn, 2013; Ma et al., 2004). Actually, there are many forms of point defects in a graphene, including the vacancies, impurities and structure distortions, etc (Banhart et al., 2011; Hashimoto et al., 2004). We just focus on the point defect of the vacancies in this study. Apparently, the simplest method for making the vacancies in a graphene is to employ the irradiation of heavy ions. Obviously, when the irradiation is active, some charges on the carbon atoms of graphene will transfer inwards or outwards, the phenomenon of which is similar to that of proceeding electron (Wang et al., 2009) or hole doping (Gierz et al., 2008) to the graphene, respectively. To simplify the calculation, we let the vacancy-defect graphene have a smallest unit cell, namely, in a highest vacancy level, the structure is depicted in Fig. 1 (a). In figure 1, we assume the magnetism in the vacancy-defect gra phenes with various vacancy concentrations have the same property and just show the different quantity. Because the serious spin frustration initially exists in the two-dimensional system (Takahashi, 1997), a magnetic graphene will be not a good candidate material for the spintronics any longer. In short, the ferromagnetism is expected to exist in the point-defect graphene, while this graphene will be suppressed by the spin fluctuation indu ced from the low dimensionality. The bi-layer graphene out of two dimensional ideal systems will suppress the spin fluctuation instead. We thus

propose to strengthen the ferromagnetism by means of increasing the dimensionality from constructing the point-defect graphene on a perfect graphene. Meanwhile, the inter-layer coupling will spontaneously be induced in the bi-layer graphene. In this study, the structure of the magnetic bi-layer graphene comprises a top layer graphene with point

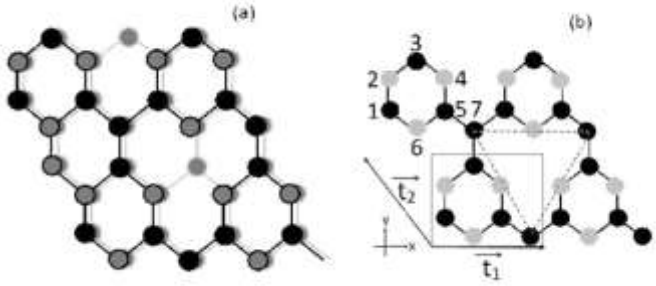

Fig. 1: (a) The structure of vacancy-defect bi-layer graphenes. (b) The unit cell of vacancy-defect graphene in the top layer of (a). There are 7 atoms as indexed in a unit cell.

defects and a perfect structured graphene on the bottom. Similar to the graphite, both layers are constructed by AB stacking to form a stable state (Aoki, Amawashi 2007). According to many experimental techniques for constructing the bi-layer system, we will not discuss the related issue especially for the theoretical frame in this study. However, the coupling between both graphene layers needs to be considered, because the ferromagnetism will be affected by the coupling. Due to the layer-layer coupling, the charge transfer will occur.

In a graphene, each carbon atom bonds with each other in sp2 configuration and results in a dangling π bond, in which an electron is restricted in the π orbit, namely, each carbon atom has a π electron. The π bond plays two roles in the conducting along the plane of each layer and the coupling with another layer, respectively. The orbital potentials of the atoms in the edge sites of vacancy defects will be relatively low, compared to other atoms, because of the truncation in the covalent bonds. Similarly, the Coulomb repulsion is reduced on these edge atoms, because their orbital spaces of electrons could extend to the vacancy sites. Due to the relatively low Coulomb repulsion on the atoms around the point defects, the doping electrons will occupy the top parts (lay) of these atoms preferentially, which makes the ferromagnetism varied. Similarly, the charge transfer occurs from the bottom layer to the top one, in which the transferred electrons will preferentially stay in these atoms too. On the contrary, in the hole doping the doped holes will approach to the atoms, instead of being adjacent to the point defects. Eventually, we investigate both effects on the ferromagnetism through different charge types of carrier doping and the charge transfer between graphene layers through this study.

2. Theoretical Description

We begin the calculation by constructing the total Hamiltonian to a matrix form which comprises four sub-matrices corresponding to four sub-Hamiltonian, including top layer of vacancy-defect graphene, bottom layer of pure graphene, and two sub-matrices in the off-diagonal sites representing for the couplings between both layers, respectively. The scale of the Hamiltonian matrix is extended to 15 × 15 for each spin carrier, indexed by σ, because each unit cell has 7 atoms in the vacancy-defect graphene and 8 atoms in the pure graphene, respectively.

The sub-Hamiltonian of the top layer of vacancy-defect graphene, H_{aa}, is

$$H_{aa} = \sum_{i,j=1}^{7} V_{i,j} c_j^{+} c_j + \sum_{i=1}^{7} (E_i c_j^{+} c_i + \frac{1}{2} \sum_{\sigma=-\frac{1}{2}}^{+\frac{1}{2}} U_i n_{i,\sigma} n_{i,\bar{\sigma}}), \tag{1}$$

where c_i and (c_i^{+}) is the annihilation (creation) operator for site i = 1, 2, ⋯ , and 7 whose relative positions [refer to Fig. 1(b)] are~r_1 = (0, 1/23),~r_2 = (0,3/2),~r_3 = (1/2, 23/3),~r_4 = (1,3/2),~r_5 = (1, 1/23), ~r_6 = (1/2, 0) and ~r_7 = (3/2, 0), respectively. The notation $V_{i,j}$ represents the nearest hopping

between the I and j sites, herein we suppose the hopping integral between the nearest neighbor sites are the same, $V_{i,j} = V$. We index the seven atoms of the unit cell around the vacancy-defect to two groups. Four atoms are in-dexed by i = 1, 3, 5 , 7. Three atoms very adjacent to the vacancy are indexed by i = 2, 4, 6. E_i is the orbital energy for each carbon atom. The last term in Eq. (1), with $n_{i,\sigma}$ and $n_{i,\bar{\sigma}}$ being the particle number operators, accounts for the Coulomb repulsion on site i with strength $U_i > 0$ which gives the elec-trons on site i carrying spin $\sigma = \pm 1/2$ to exert repulsive forces to spin $\bar{\sigma} = -\sigma$. In order to decouple the four operators of Coulomb interaction to two operators of that, we take the mean field approximation, $U_i n_{i,\sigma} n_{i,\bar{\sigma}} = U_i \langle n_{i,\sigma} \rangle n_{i,\bar{\sigma}} + \langle n_{i,\bar{\sigma}} \rangle n_{i,\sigma} - U_i \langle n_{i,\sigma} \rangle \langle n_{i,\bar{\sigma}} \rangle$. The whole system of infinite two-dimension is formed by the translation vectors $\vec{r}_1 = (2,0)$ and $\vec{r}_2 = (-1, \sqrt{3})$ i.e., the total sub-Hamiltonian is obtained by repeating the unit-cell Hamiltonian (1) with displacements $n\vec{r}_1 + m\vec{r}_2$ where n and m are integers.

The sub-Hamiltonian in the bottom layer of pure graphene, H_{bb}, is similar to eq. (1) with the same unit vectors instead of the vacancy sites. The off-diagonal sub-matrices in the whole Hamiltonian matrix, H_{ab} and H_{ba}, are the coupling interactions between both layers. In the coupling matrices, we consider the couplings of the nearest neighbor and the secondary nearest one between atoms from both layers. The nearest neighbor coupling V_p is coupling for the top to top atoms. The secondary nearest neighbor coupling V_G is the coupling from the atom to next nearest neighbor atoms. Consequently, these four sub-matrices form the matrix of the total Hamiltonian,

$$H = \begin{pmatrix} H_{aa} & H_{ab} \\ H_{ba} & H_{bb} \end{pmatrix} \tag{2}$$

Since the system is unit-cell translation invariant, the Hamiltonian can be represented in the momentum k and the total Hamiltonian on a basis of the crystal momentum k is block diagonal. For brevity, subsequently, we will use $n_{i,\sigma}$ to notate $\langle n_{i,\sigma} \rangle$, the quantum-thermal average number of the particle occupation.

To determine the occupation $n_{i,\sigma}$, we consider minimizing the free energy,

$$F = -\frac{1}{N} k_B T \sum_{\alpha,\vec{k},\sigma} \ln(1 + e^{(\mu - E_{\alpha,\sigma})/k_B T}) - \frac{1}{2N} \sum_{i,\sigma} U_i n_{i,\sigma} n_{i,\bar{\sigma}}, \tag{3}$$

subject to the initial constrain of half-filling (i.e., occu pation number on each atomic π orbit is one) before the charge doping from the heavy ions bombardment and the charge transfer between the graphenes

$$n_{i,\sigma} + n_{i,\bar{\sigma}} = 1.$$

$E_{\alpha,\sigma}$ is the α-th eigenvalues of the spin-σ Hamiltonian (1), μ is the chemical potential determined by

$$\sum_{i,\sigma} n_{i,\sigma} = \sum_{\alpha,\sigma} f_D(E_{\alpha,\sigma}) = 15, \tag{4}$$

with $f_D(\varepsilon) = \{1 + exp[(\varepsilon - \mu)/(k_B T)]\}^{-1}$ being the Fermi-Dirac distribution function , μ the chemical potential, k_B the Boltzmann constant, and T the temperature. The problem of minimization can be solved by adopting the Lagrange multiplier to find appropriate seven λ_i and fourteen $n_{i,\sigma}$ and $n_{i,\bar{\sigma}}$ that satisfy, fourteen (i = 1, 2, ⋯ 15 and $\sigma = \pm 1/2$)

$$\nabla F = \sum_i \lambda_i \nabla g_i. \tag{5}$$

equations with $\nabla = \sum_{i=1}^{15} \frac{\partial}{\partial n_{i,\sigma}} \hat{e}_{i,\sigma}$ and $\hat{e}_{i,\sigma}$ being the unit vector, and seven (i = 1, 2, ⋯ 15)

$$g_i = (n_{i,\sigma} + n_{i,\overline{\sigma}} - 1) = 0. \quad (6)$$

equations. In the present case, further simplification can b e obtained by eliminating λ_i in Eq. (5) to give seven (i = 1, 2, ⋯ 15)

$$\frac{\partial F}{\partial n_{i,\sigma}} = \frac{\partial F}{\partial n_{i,\overline{\sigma}}} \quad (7)$$

equations. We note that the minimization objective F is a function of $n_{i,\sigma}$and $n_{i,\sigma}$, because F is a function of μ determined by the $n_{i\sigma}$-dependent Eq. (4), and $E_{\alpha,\sigma}$ is obtained by solving the eigen problem of the $ni\sigma$-dependent Eq. (2); the partial derivative in Eq. (7) thus reads, $\partial F/\partial nj,\sigma = \sum i,k,\sigma fD(Ei,\sigma)[\partial Ei,\sigma(k)/\partial nj] - Ujnj,\sigma$. The seven equations in Eq. (7) together with the seven equations in (6) is sufficient to solve the fourteen ni,σ and ni,σ. The magnetization of each lattice site is eventually determined by $m(i) = (ni,1/2 - ni,- 1/2)/2$, i.e., one half of the difference between opposite spin carrier numbers on site i. It is worth mentioning that the spin quantum fluctuation is ignored in this present meanfield approach, while this fluctuation can be reduced if the point-defect graphene couples with a defect-free graphene. Similarly, in treating the doping cases, either negative or positive, we just need to modify the total carrier density and each site density in eq. (4) and eq. (6), respectively.

3. Results and Discussions

According to the previous work we presented, the ferromagnetism in a single layer honeycomb structure with vacancy defects appears around the vacancy sites and signifi cantly exist on sites 2, 4, 6 and 7th in a unit cell. The magnetization on sites 1, 3 and 5th sites will be ignored, even though a very small antiferromagnetism occurs. We have confirmed that the ferromagnetism originate s from the interior edges (i.e., 2, 4, 6 and 7th sites) which provides the edge bands intersecting the Fermi-level and the ferromagnetism shows up under large enough on-site Coulomb repulsions. In the bi-layer graphene, the structure as shown in Fig. 1 (a), the inter-layer coupling will be spontaneously induced. There are two different couplings, V_p and V_G, the nearest neighbor and the secondary nearest neighbor from top layer sites to bottom layer sites, respectively. We suppose that V_P should be larger than V_G because of shorter site to site distances. In this paper we set V_P/V_G is 4/3 a rough estimation by their distance ratios. The magnetic properties in the bi-layer case are similar to the single vacancy-defect layer. The ferromagnetism only exits on the vacancy-defect top layer, as shown in Fig. 2. Interestingly, by the calculations we discover these inter-layer couplings will suppress the ferromagnetism, as shown in Fig. 3. In particular, all ferromagnetism on different sites will disappear with the same critical coupling strength. In comparison with the result of fig. 2, the increase of coupling is equivalent to the decrease of Coulomb repulsion. The result is rational because the carriers on the edge states in the vacancy-defect layer gain an extra degree of freedom through the layer-layer couplings and further move to the bottom layer, which reduces the effective Coulomb repulsion on carriers. Therefore, there is a trade-off between the reduction of the spin fluctua tion and the increase of the internal couplings. Furthermore, this result also implies the fact that the ferromagnetism will decrease with the increase of applying pressure, because the couplings increase through the reduction of the site to site distances.

Regarding the experimental issue, we propose the vacancy defects could be created by the heavy ions bombardment. During the bombardment, some charges, either negative or positive, are transferred to the sample from the incident heavy ions. We also suppose that the distribution of the transferred charges be uniformly distributed on every atomic site of the bi-layer sample. Based on this assumption, we restrict the carrier density on every site to be the same in our calculations. The calculation results indicate that the external charge transfer (or called as charge doping) makes the magnetization decrease in either negative or positive charge transfer. In fact, this result further implies that every charge doping process to the ferro-magnetic graphene-like samples could reduce the ferromagnetism. Actually, we can take a close inspection to the result that the maximum

ferromagnetism exists in a very small n doping, as shown in Fig. 4 , and

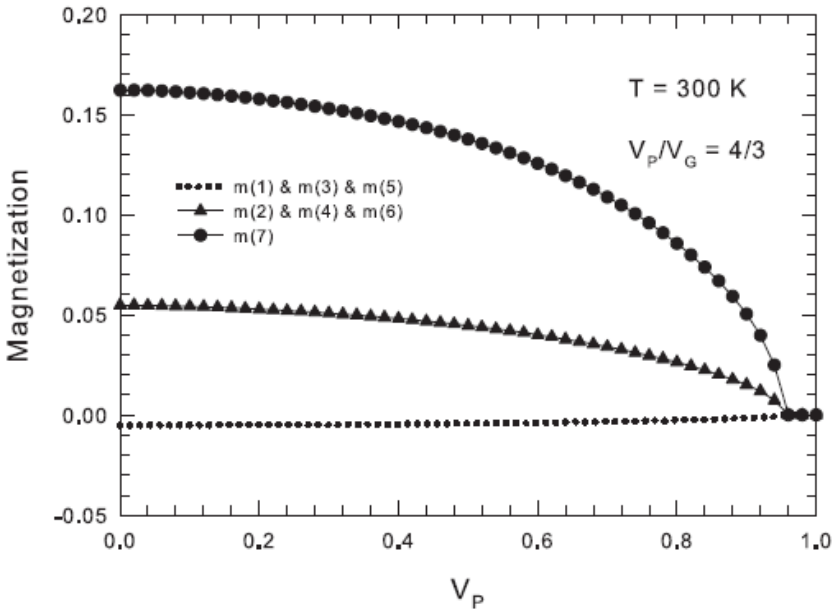

Fig. 2: The magnetization of each atomic site in the unit cell of vacancy-defect graphene as a function of the nearest neighbor coupling, V_P, at room temperature, 300 K.

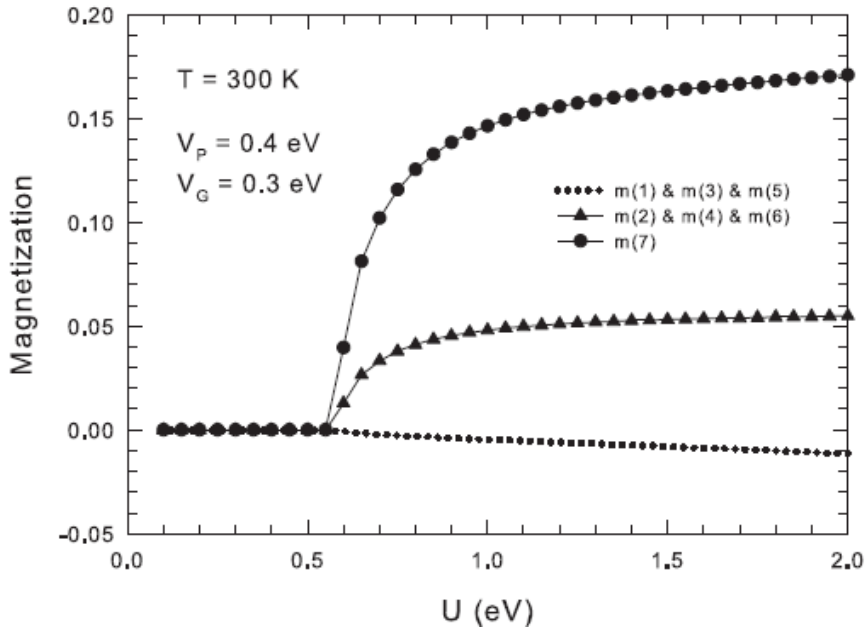

Fig. 3: The magnetization of each atomic site in the unit cell of vacancy-defect graphene as a function of Coulomb repulsion, U, at room temperature, 300 K. The nearest neighbor and the secondary nearest neighbor couplings, V_P and V_G, are 0.4 and 0.3 eV, respectively.

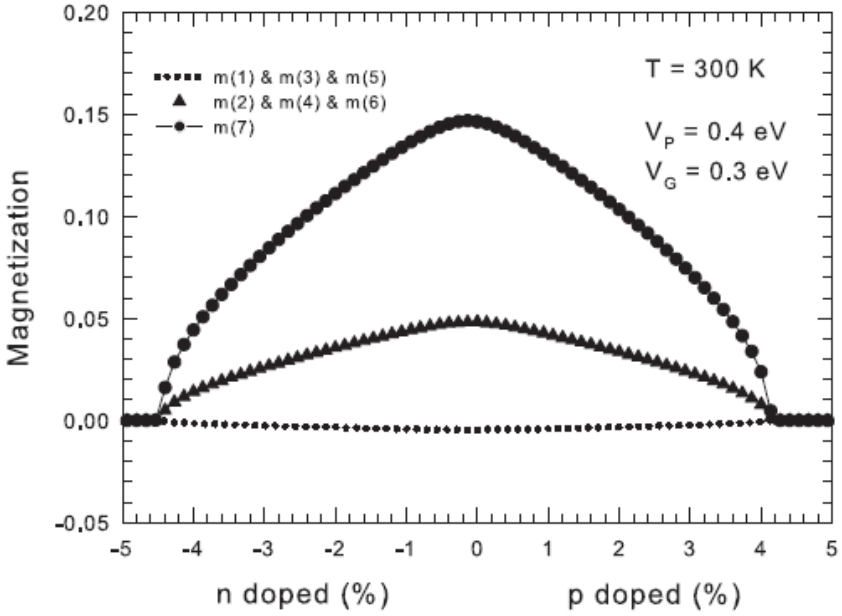

Fig. 4: The magnetization of each atomic site in the unit cell of vacancy-defect graphene as a function of external carriers doping ratio at room temperature 300 K. The nearest neighbor and the secondary nearest neighbor couplings, V_P and V_G, are 0.4 and 0.3 eV, respectively. The electron (hole) doping is negative (positive).

will find the fact, as our understanding before, that the ferr omagnetism of the vacancy-defect graphene orig-inates from the edge states with different spin splitting. The Fermi-level mostly intersects the edge bands of majority spin. The edge bands of minority spin are just slightly above the majority bands. For this reason, the small increase of the Fermi-level, i.e., n doping, before touching the minority edge bands, the density of the majority spin increases. As the n carriers keep increasing, the Fermi-level will intersect the minority edge bands, which makes the ferromagnetism begin to decrease obviously. On the contrary, in the small p doping, the Fermi-level decreases, while the spin density of the majority edge bands decreases, which leads to the decrease of the ferromagnetism. Except the very small n doping, the ferromagnetism decreases with the increase of charge doping, in either negative or positive and disappears eventually. The ferromagnetism decreases owing to the minority spin bands filling with the in crease of charge doping. In particular, the results of this study show that the doping effect on the suppression of ferromagnetism is very sensitive. It is approximately 4 % doping to completely suppress the ferromagnetism. This result is clearly derived from the fact that the ferromagnetism of the vacancy-defect graphene mostly originates from the spin-split edge bands, since these edge bands are very close to the Fermi-level and lead sensitiveness to to carrier doping.

On the other hand, the internal charge transfer is a possible approach different from the external charge transfer as mentioned above. it is worth noting that the charge carriers only transfer between both layers. We suppose some cases could induce the internal charge transfer. For instance, once the internal energy between both layers is out of balance, it will reconstruct vacancy defects. If the transferred charges are also uniformly distributed to every atomic site, the calculating results will be very different from the external cases. The magnitude of the magnetization is almost unchanged, as shown in Fig. 5. This result reconfirms that the ferromagnetism is closely related to the edge bands and Fermi-level. Since in the internal charge transfer the total carriers are not changed, the result leads to the Fermi-level unchanged and a constant ferromagnetism.

In the summary, the bi-layer vacancy-defect graphene containing vacancies in the top layer of graphene and a perfect graphene, which is regarded as a bottom layer with showing the ferromagnetism on every atomic site under a proper on-site Coulomb repulsion. The ferromagnetic magnetization only exists on the interior edges around the vacancy sites. Our calculation results reveal the fact that the internal coupling between both layers suppresses the ferromagnetism, which leads to a trade-off between the increase of dimensionality.

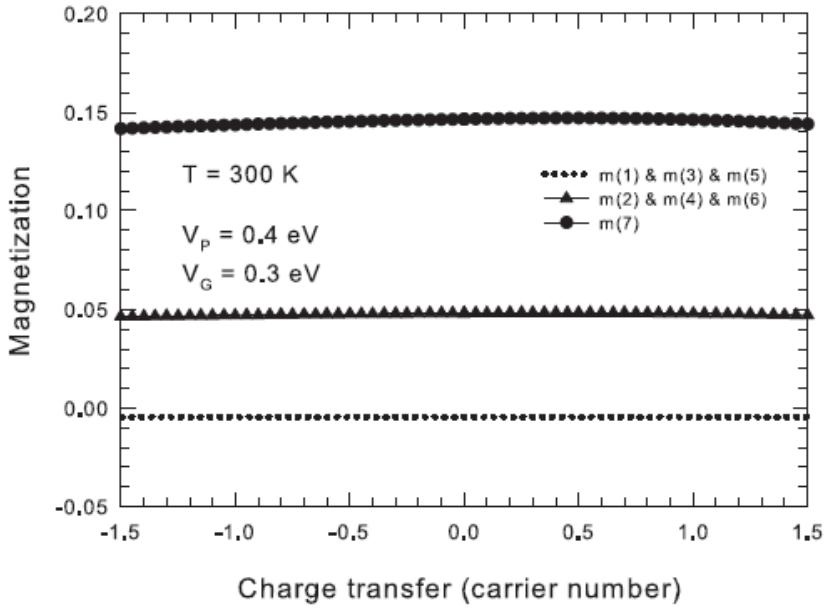

Fig. 5: The magnetization of each atomic site in the unit cell of vacancy-defect graphene as a function of internal charge transferred carriers at room temperature 300 K. The nearest neighbor and the secondary nearest neighbor couplings, V_P and V_G, are 0.4 and 0.3 eV, respectively. The positive (negative) charge transfer represents carriers transferring from bottom layer (top layer) to top layer (bottom layer).

The coupling stabilizes the magnetization and causes the decrease of the magnetization. The external charge transfer or called charge doping, sensitively reduces the ferromagnetism in either negative or positive doping. On the contrary, the internal charge transfer between both layers hardly makes any change to the ferromagnetism.

Acknowledgment

We would like to thank the support by the Republic of China National Science Council Grant No. NSC-101-2112-M-390-001-MY3 and No. NSC-102-2112-M-845-001-MY3. The hospitality of the National Center for Theoretical Sciences, Taiwan, where the work was initiated, is gratefully acknowledged.

References

Avouris, Phaedon Zhihong Chen and Vasili Perebeinos, (2007) Carbon-based electronics, Nature Nanotechnology **2**, 605 – 615.

Castro Neto, A. H., F. Guinea, N. M. R. Peres, K. S. Novoselov and A. K. Geim, (2009) The electronic properties of graphene, Rev. Mod. Phys. **81**, 109V162.

Novoselov, K. S. A. K. Geim, S. V. Morozov, D. Jiang, M. I. Katsnelson, I. V. Grigorieva, S. V. Dubonos and A. A. Firsov, (2005) Two-dimensional gas massless Dirac fermions in graphene, Nature **438**, 197-200.

Tombros, Nikolaos, Csaba Jozsa, Mihaita Popinciuc, Harry T. Jonkman and Bart J. van Wees, (2007) Electronic spin transport and spin precession in single graphene layers at room temperature, Nature **448**, 571-574.

Haugen, Havard, Daniel Huertas-Hernando, and Arne Brataas, (2008) Spin transport in proximity-induced ferromagnetic graphene. Phys. Rev. B **77**, 115406

Yazyev, Oleg V., M. I. Katsnelson, (2008) Magnetic correlations at graphene edges: basis for novel spintronics devices. Phys. Rev. Lett. **100**, 047209.

Kan, Erjun Zhenyu Li, and Jinlong Yang, (2008) Magnetism in graphene systems, NANO **3**, 433.

Dugaev, V. K., V. I. Litvinov, and J. Barnas, (2006) Exchange interaction of magnetic impurities in graphene, Phys. Rev. B **74**, 224438

Santos, E. J. G., D. Sanchez-Portal, and A. Ayuela, (2010) Magnetism of substitutional Co impurities

in graphene, Realization of single π vacancies, Phys. Rev. B 81, 125433
Wu, M., En-Zuo. Liu, J. Z. Jiang, (2008) Magnetic behaviour of graphene absorbed with N,O, and F atoms: A first principles study, Appl. Phys. Lett. **93**, 082504,
Palacios, J. J., J. Fernandez-Rossier, (2008) Vacany-induced magnetism in graphene and graphene ribbons, Phys. Rev. B **77**, 195428
Esquinazi, P., D. Spemann, R. Hohne, A. Setzer, K.-H. Han, and T. Butz, (2003) Induced magnetic ordering by proton irradtion in graphite, Phys. Rev. Lett. **91**, 227201
Nair, R. R. M. Sepioni, I-Ling Tsai, O. Lehtinen, J. Keinonen, A. V. Krasheninnikov, T. Thomson, A. K. Geim, and I. V. Grigorieva, (2012) Spin-half paramagnetism in graphene induced by point defects, Nature Physics 8, 199V202
Joly, Joseph, V. L., Manabu Kiguchi, Si-Jia Hao, Kazuyuki Takai, and Toshiaki Enoki, et al, (2010) Obsvertaion of magnetic edge state in graphene nanoribbons, PHYS. REV. B **81**, 245428
Uchoa, Bruno, Valeri N. Kotov, N. M. Peres, and A. H. Castro Neto, (2008) Localized magnetic states in graphene, Phys. Rev. Lett. 101, 039903
Fujita, Mitsutaka, Katsunori Wakabayashi, Kyoko Nakada and Koichi Kusakabe, (1996) Peculiar localized state at zigzag graphite edge, J. Phys. Soc. Jpn. **65**, 1920-1923
Kumazaki, Hidek, and Dai S. Hirashima, (2008) Local magnetic moment formation on edges of graphene, J. Phys. Soc. Jpn. **77**, 044705
Son, Young-Woo, Marvin L. Cohen, and Steven G. Louie, (2006) Half-metallic graphene nanoribbons, Nature **444**, 347-349
Sun, Shih-Jye J. (2013) Magn. Magn. Mat. **344**, 39V43
Yuchen, Ma, P. O. Lehtinen, A. S. Foster and R. M. Nieminen, (2004) Magnetic properties of vacancies in graphene and single-walled carbon nanotubes, New J. Phys. **6**, 68
Banhart, Florian, Jani Kotakoski, and Arkady V. Krasheninnikov, (2011). ACS Nano, **5**, 26V41
Hashimoto, Ayako, Kazu Suenaga, Alexandre Gloter, Koki Urita, and Sumio Iijima, (2004) Direct evidence for atomic defects in graphene layers, Nature **430**, 870-873
Wang, Xinran, Xiaolin Li, Li Zhang, Youngki Yoon, Peter K. Weber, Hailiang Wang, Jing Guo, Hongjie Dai, (2009) N-doping of graphene through electrothermal reactions with ammonia, Science **324**, 768-771
Gierz, Isabella Christian Riedl, Ulrich Starke, Christian R. Ast, and Klaus Kern, (2008) Nano Lett. **8**, 4603V4607
Takahashi, Yoshinori (1997). J. Phys.: Condens. Matter **9**, 10359V10372
Aoki, Masato, Hiroshi Amawashi, (2007) Solid State Comm. **142**, 123V127